ELECTRICAL CONDUCTIVITY OF HYBRID/PATTERNED NANOCOMPOSITES FILMS

R. D. Farahani, D. Therriault*
Laboratory for Multiscale Mechanics, Center for applied research on polymers (CREPEC), École Polytechnique de Montreal, Montreal (QC), Canada
* Corresponding author (daniel.therriault@polymtl.ca)
Keywords: *Nanocomposite, conductivity, heterogeneous dispersion*

1 Abstract
Here, with the aim at improving electrical conductivity of carbon nanotube/polymer nanocomposite films in a given nanofiller concentration, two different approaches were studied: nanomaterials localization through nanocomposite patterning and hybrid nanocomposite systems. In the first approach, nanocomposite meshes were fabricated through the directed deposition of the nanocomposite filaments on a substrate using the UV-assisted direct-write technique. The pore spaces between the filaments were then filled with the neat polymer to create a thick film. A similar nanocomposite film with the same thickness and amount of nanotubes was also fabricated with a homogeneous distribution for comparison purposes of their electrical properties. The film composed of nanocomposite mesh showed higher electrical conductivity (by two orders) compared to a film with homogeneous nanotube distribution. In the second approach, an additional nanoinclusion, either graphene or silver nanowires was introduced to the nanotube/polymer nanocomposite in order to study the synergetic effects of two nanofillers (50/50 by weight with total concentration of 1wt.%) in the resulting hybrid (ternary) system. The second approach did not show an improved electrical conductivity at least at these low nanofillers concentrations.

2 Introduction
Electrically conductive nanocomposites using nanomaterials such as carbon nanotubes (CNTs), graphene, and metallic nanowires incorporated into polymer matrices feature advanced multifunctional properties for a wide variety of applications in aerospace and microelectronics [1-7]. In particular, in conventional aerospace composite structures, a copper mesh is bonded on the outer surface of the structure to provide a conductive path serving as protection against lightning strike [2]. The aerospace industry desires to replace these heavy metal meshes with lighter materials like nanotube-polymer nanocomposites while preserving the conductivity requirement. However, until now, most of the researches undertaken on using nanocomposites as conductive surface have been limited to the use of nanocomposite films with uniform filler distribution [5,7,8].

The electrical conductivity of polymer-based nanocomposites involves the formation of conductive nanofiller percolation networks in the polymer matrix. The increase of the conductivity can be attributed to the formation of conductive pathways when the filler content exceeds a critical volume fraction. This critical concentration of the conductive additive (e.g., CNTs) is named the percolation threshold. In general, for additive concentrations below the percolation threshold, the electrons must travel through several large zones of insulating polymer matrix between the neighboring conductive nanotubes defined as electron tunneling. When the percolation networks are formed (above the percolation threshold), electrons conduct predominantly along the conductive nanotubes and move directly from one nanotube to the next. The importance of tunneling effect gradually decreases with increasing the nanotube loadings by providing more conductive paths [9].

The percolation threshold for conductive particles embedded in an insulated polymer is very sensitive to the geometry of the fillers and their spatial arrangements in the matrix. A decrease in electrical resistivity with an increase in filler content is attributed to the probability of the fillers to contact each other [9]. The characteristics and properties of the fillers themselves (e.g., aspect ratio, specific surface area, and surface conductivity), their dispersion and interfacial interaction between the nanotubes and polymer matrix are parameters influencing the composite conductivity [3,10]. The percolation threshold can be achieved at lower filler

concentrations by using high aspect ratio (i.e., length/diameter) fillers. Any kind of treatment such as shear mixing, sonication and functionalization can damage the fillers and reduce the aspect ratio of the nanotubes which will lead to an increase of the percolation threshold [10].

Recently, the optimized dispersion/distribution status of nanofillers has been of a great interest in order to increase the electrical conductivity of nanocomposites at a given concentration. Hybrid (ternary) system having two different nanofillers have been reported to represent enhanced electrical conductivity through the synergy between two different nanofillers [11,12]. A heterogeneous distribution has been demonstrated to achieve higher conductivities at lower nanofiller loadings compared to homogeneous distribution [2,13]. Double percolation, i.e., confining nanofillers in any one of the phases of a biphasic polymer, and the creation of repulsive forces between nanofillers and the host polymer (e.g., polar/non-polar) were demonstrated as efficient techniques [13].

Here, we present two different approaches to improve the conductivity of polymer-based nanocomposites. The first method is based on the utilization of the ultraviolet-assisted direct-write (UV-DW) technique [3,14] for the fabrication of a conductive nanocomposite mesh. This mesh was electrically compared with a nanocomposite film of the same overall size and same amount of nanofillers but uniformly distributed through the fabricated films. The second approach is to form a ternary nanocomposite using an additional filler in order to investigate the synergetic effect of different fillers for improving their dispersion and the electrical conductivity of the resulting hybrid nanocomposites.

3 Experimental details

3.1 Nanomaterials characterization

Three different nanomaterials were used in this study: multi-walled carbon nanotube (MWCNT) produced by catalytic CVD method was purchased from Skysprings Nanomaterials Inc. The diameter and length of the MWCNTs were 10-20 nm and 5-30 µm, respectively. Graphene nanopowder having average flake thickness of 8 nm was purchased from Graphene Supermarket. Silver nanowires were also provided from Nanostructured & Amorphous Materials Inc. with the diameter and length of 227 nm and 6.1 µm, respectively.

The nanomaterials were observed by field emission scanning electron microscopy using a Jeol JSM-7600TFE (FESEM, 5 kV) microscope and also by transmission electron microscopy (TEM) using a Jeol JEM-2100F (FEG-TEM, 200 kV) microscope. Raman spectra were acquired at room temperature in the 100-2000 cm^{-1} spectral region under ambient conditions using a back-scattering geometry on a microRaman spectrometer (Renishaw Imaging Microscope Wire TM) with a 50× objective to focus the laser beam on the sample. The sample excitation was performed by using a 514.5 nm (2.41 eV) line from an air cooled Ar+ laser. The MWCNTs and graphene sheets were also characterized by *X*-ray photoelectron spectroscopy (XPS, Escalab 220i-XL system, VG instruments) using the monochromatic Al Ka radiation as the excitation source (1486.6 eV, full width at half-maximum of the Ag 3d5/2 line = 1 eV at 20 eV pass energy) in order to assess their quality and possible presence of functional groups.

3.2 Nanocomposite preparation

The nanocomposites were prepared by blending a special one-component dual cure (ultraviolet/heat curable) polymer resin (NEA 123MB, Norland Product Inc.) and nanomaterials, either only MWCNTs or its combination with the second nanofiller (i.e., graphene or silver nanowire) at different loadings using ultrasonication method. The desired amount of nanofillers were first dispersed in dichloromethane (DCM, Sigma-Aldrich) by bath ultrasonication (Ultrasonic cleaner 8891, Cole-Parmer) for 30 min. The resin was then mixed with the nanotube suspension in DCM over a magnetic stirring hot plate (model SP131825, Barnstead international) at 40°C for 4 h. The residual solvents were evaporated by heating the mixtures at 30°C for 12 h and at 40°C for 24 h in a vacuumed-oven (Cole Parmer).

3.3 Fabrication of nanocomposite mesh and film

The UV-DW technique (Fig. 1a) was used to fabricate nanocomposites meshes inspired by the conventional copper mesh geometry in order to confine the conductive nanofillers in a defined path and facilitating their direct contact. The UV-DW platform is composed of a computer-controlled robot (I & J2200-4, I & J Fisnar) that moves a dispensing apparatus (HP-7X, EFD) and a UV light-emission set-up along the *x*, *y* and *z* axes. The mesh was fabricated by extruding the nanocomposite suspension through a micro-nozzle (5127-0.25-B,

EFD, *ID* = 150 μm) over a glass substrate. The mesh was 50 mm long and 10 mm wide (Fig. 1b). The structure was in-situ cured using UV exposure (LED, NCSU033A, Nichia, having a wavelength centered at 365 nm) while being extruded. The pore spaces between the filaments were then filled with the neat polymer, resulting in a thick film consisting of the nanocomposite mesh embedded into the neat polymer. To assess the effect of nanocomposite patterning, a thick film of nanocomposite of similar dimensions (a calculated thickness) of the mesh structure was also fabricated (Fig. 1c). The nanofiller loading were normalized over structures' volume so that the amount of MWCNT in the nanocomposite mesh and film were equal. A nanocomposite film containing 5 wt.% of MWCNTs was also fabricated for comparison purposes. All the samples were first put under illumination of a UV lamp (Cole-Parmer) for 30 min for pre-curing, followed by post-curing in the oven at 90 °C for 3 h.

3.4 Nanocomposite morphological and electrical characterization

For optical imaging purposes, a ~20 μm-thick film of the nanocomposite was fabricated by UV-DW. The quality of the mixture was observed for the cured nanocomposite film using an optical microscope (BX-61, Olympus) and image analysis software (Image-Pro Plus6, Media Cybernetics).

The electrical properties of the nanocomposite mesh and film were characterized using a Keithley 4200 semiconductor parametric analyzer (MM 2000 probe station) between two ends of the samples. These two ends were silver-coated for ensuring proper electrical contact and served as electrodes, as shown in Figure 1c.

4 Results and Discussion

4.1 Nanomaterials characterization

Figure 2 shows typical SEM and TEM images of the nanomaterials used in this study. According to the supplier as well as our results, the MWCNTs have been purified, although few impurities (i.e., dark particles in the TEM image) are also observed. These are likely some residual catalyst nanoparticles, which were not entirely digested during the possible purification step. The MWCNTs exhibit a diameter in the 10-20 nm range and lengths reaching up to few tens of microns. The graphene sheets are stacked due to the weak van der Waals interaction while the individual silver nanowires can be easily seen in the SEM and TEM images.

Raman spectroscopy of MWCNTs and graphene provides information on the quality of structural ordering. In Figure 3a, the peaks located in the 1300-1600 cm^{-1} range; the D-band (1350 cm^{-1}) and the tangential stretching G-band (1600 cm^{-1}), are typical fingerprints of MWCNTs and graphene. The G/D ratio is generally used to qualify the degree of purity of these nanostructures. Here, the G/D ratio of MWCNTs and graphene are found to be ~1.1 and ~12, respectively, which indicate their quality are relatively high compared to those reported in the literature [15]. This is further supported by XPS measurements shown in Figure 3(b). The main C 1s core level peak that arises from the C=C bonds is narrow in both samples at 285 keV. A few very weak peaks are also observed which might be attributed to the functional groups, possibly created during the purification step. Based on all the above results, it is fair to assume that the possible purification process by the supplier did not affect the structural quality of these carbonaceous structures which is the ideal case for electrical conductivity improvement.

4.2 Nanomaterials dispersion

Figure 4 shows typical optical micrograph of nanocomposite films, either single filler or hybrid ones with different nanofillers type and concentration. The bright regions represent the surrounding polymer while the observed dark spots are thought to be nanotubes aggregates and/or graphene sheets. The aggregates represent different sizes up to ~10 μm in diameter, although majority of them have smaller sizes down to ~1 μm in diameter). A very high degree of dispersion is not observed as expected since ultrasonication is found as an inefficient method to well disperse the nanofillers in the polymer matrix. Moreover, it is clearly hard to reach high degree of dispersion without the help of the functional groups. It should be mentioned that for the sake of electrical properties improvement, there is no need to uniformly disperse the fillers and also the fillers chemical functionalization should be avoided [15].

Figure 4a shows an optical image of nanocomposite film containing 5 wt.% of MWCNTs. The MWCNT aggregates with different sizes are observed which seem to form conductive pathways. The MWCNT

aggregates are less compact and farther from each other at lower concentration, as shown in Figure 4b. The conductive paths might be still created in this case, assuming the individual MWCNTs cannot be observed by the optical microscopy. In the absence of second filler, MWCNTs tend to highly aggregate and therefore a visible percolation network cannot be observed. The average size of MWCNT aggregates slightly diminished in the presence of the additional nanofillers, either graphene or silver nanowires (50/50 by weight with total concentration of 1wt.%), as can be seen in Figures 4c and 4d. This suggests that the addition of the second filler confer a synergetic effect on the MWCNTs dispersion [11,12]. This microstructure is a favorite case for the sake of mechanical properties improvement but not necessarily for the enhancement of electrical performance of the resulting hybrid nancomposites.

4.3 Electrical characterization

4.3.1 First approach: Nanocomposite patterning

Figure 5 shows the *I-V* curves of the nanocomposite mesh and films. The electrical conductance of the nanocomposite film containing 1 wt.% uniformly-distributed MWCNTs is found to be as low as ~3.3 × 10^{-5} $S.m^{-1}$. This value dramatically increased to ~2 × 10^{-3} $S.m^{-1}$ (by two orders) for the films composed of nanocomposite mesh. The conductivity improvement can be interpreted by understanding the contribution of two main nanocomposite electrical conductivity mechanisms which are nanotubes' direct contact and/or electron tunneling between neighboring nanotubes in proximity. Since the amount of nanotubes is equal in both the nanocomposite mesh and the film, the nanocomposite patterning permitted to confine MWCNTs in a desired pattern, and thus enhancing the probability of contact points through which electrons are transferred and also decrease the distance of adjacent nanotubes. For the nanocomposite mesh, the direct contact is believed to be dominant. This is further confirmed by comparing the electrical conductivity of the nanocomposite mesh and nanocomposite film containing 5 wt.% of MWCNTs. The electrical conductivity of the film (uniform distributed 5 wt.% nanotubes) is slightly above that of the nanocomposite mesh using only 1 wt.% MWCNTs. It should be mentioned that the electrical conductivity of nanocomposites does not increase too much above certain nanotube concentrations.

In addition to other parameters (e.g., aspect ratio and surface treatment) influencing the electrical conductivity of polymer nanocomposites, the nanofiller dispersion/distribution seems to play an important role regarding the maximum achievable conductivity. Although there is an argument in the literature [11,12] on the dispersion effect on nanocomposite electrical conductivity, many reports including the present paper suggest that the highest conductivities are not necessarily achieved at the best filler dispersion [15]. This might be due to the fact that a good dispersion can lead to the formation of an insulating polymer layer around the conductive fillers, compromising electron transfer in the fillers percolation paths. It is worth noting that the nanocomposite mesh manufactured here not only helped for the enhancement of electrical conductivity, but also has high potentials (at higher filler loadings) for electromagnetic interference (EMI) shielding applications representing several advantages such as lightweight, corrosion resistance, flexibility, and cost-effective compared to conventional metallic based materials [4,13].

4.3.2 Second approach: Hybrid nanocomposite systems

Figure 6 represents the electrical conductivity behavior of the binary (MWCNTs/polymer nanocomposites) and the ternary (MWCNTs/second nanofiller/polymer nanocomposites) films having a total 1 wt.% of nanoinclusions, 0.5wt.% each. The highest conductivity is observed for the binary nanocomposite systems and decreased with the addition of the second nanofiller. These results are not consistent with some other works reported in the literature in which the incorporation of a second filler simultaneously improved the dispersion as well as the electrical conductivity. As shown in Figure 4, the nanotube dispersion was improved by the addition of the graphene and the silver nanowire, however, the electrical conductivity decreased. This supports our claim which indicates the best dispersion not necessarily leads to highest conductivities. Another contribution might come from the nanofillers concentration. Since the MWCNTs and the graphene represent different physical behavior (i.e., different aspect ratio and geometry), the graphene sheets might interfere the percolation pathways of the MWCNTs while the their concentration (i.e., now 0.5wt.%) might be close to the concentration threshold. It is well-known that at the vicinity of the concentration

threshold, electrical conductivity may vary several orders. Therefore, it might be concluded that the formation of a hybrid structure between two different types of nanofillers could lead to synergetic effects in network formation, thus improving the electrical conductivity at the nanofiller concentration a little far above the concentration threshold, although it is not experimentally verified here.

The same mechanism may be responsible for the decrease of the electrical conductivity of the MWCNTs/silver nanowires/polymer hybrid systems. In addition, the total volume concentration of nanofillers in this ternary system is much lower than that of the binary system, since the weight density of the silver is much higher than that of the MWCNTs. Another contribution may come from the huge difference between the fillers aspect ratio which are ~ 27 and ~ 1000 for the silver nanowires and MWCNTs, respectively. Therefore, higher silver nanowire concentrations are needed for the creation of conductive pathways. As future work, the effect of filler concentrations will be systematically studied and compared with those in the literature.

5 Conclusion

Here, in order to achieve higher electrical conductivity in a given nanotube concentration, two different approaches were studied: 1. Conductive nanomaterials localization through nanocomposite patterning and 2. Fabrication of hybrid nanocomposite films in a ternary system with the presence of an additional filler. The patterned nanocomposite mesh fabricated using the first approach showed significantly higher electrical conductivity (by two orders) compared to the similar nanocomposite film with the same thickness and amount of nanotubes, however, a uniformly situated nanotubes (i.e., homogeneous distribution). The utilization of higher nanotube loadings, coating them with metals followed by metal sintering (minimizing contact resistance), and the use of metallic nanofillers may enable to achieve high electrical conductivity required for many aerospace applications. In the second approach, a better dispersion was achieved when the additional nanofiller, either graphene or silver nanowires was incorporated to the MWCNTs/polymer nanocomposites, however, representing lower electrical conductivities. To take advantage of synergy of two nanofillers for electrical conductivity improvement, higher loading of both fillers through which the conductive network can be formed is required.

Depending on targeted applications, each approach may offer advantages over the other one. Although the patterning approach showed very promising results, the hybrid systems might be preferred for some applications due to their ease of fabrication and their cost-effectiveness. For instance, the patterning approach may be only applicable for the fabrication of small-size devices in microelectronics, but hybrid system could be easily applied for the fabrication of huge composite structures in aerospace applications.

References

[1] Y. Ear and E. Silverman "Challenges and opportunities in multifunctional nanocomposite structures for aerospace applications". *MRS Bull*, Vol. 32, No. 4, pp 328–34, 2007.

[2] M. C. G. Corporation, "Strikegrid™ Continuous Expanded Aluminum Foil (CEAF)", 2005.

[3] R. D. Farahani, H. Dalir, V. Le Borgne, L. A. Gautier, M. A. El Khakani, M. Lévesque and D. Therriault "Direct-write fabrication of freestanding nanocomposite strain sensors" *Nanotechnology*, vol. 23, p. 085502, 2012.

[4] M. H. Al-Saleh, G. A. Gelves, and U. Sundararaj, "Copper nanowire/polystyrene nanocomposites: Lower percolation threshold and higher EMI shielding" *Composites: Part A*, Vol. 42, pp 92-97, 2011.

[5] T. W. Chou, C. Li and E. Thostenson, "Sensors and actuators based on carbon nanotubes and their composites: A review" *Compos. Sci. Techno.* Vol. 68, No. 6, pp 1227-49, 2008.

[6] M. L. Culpepper and M. A. Cullinan, "Carbon nanotubes as piezoresistive microelectromechanical sensors: Theory and experiment" *Physical Review B* Vol. 82, No. 11, pp 1-8, 2010.

[7] Y. B. Park, G. T. Pham, G. T. Pham, Z. Liang, C. Zhang and B. Wang, "Processing and modeling of conductive thermoplastic/carbon nanotube films for strain sensing" *Composites Part B-Engineering* Vol. 39, No. 1, pp 209-216, 2008.

[8] L. Liu and J. C. Grunlan, "Clay Assisted Dispersion of Carbon Nanotubes in Conductive Epoxy Nanocomposites" *Adv. Funct. Mater*, Vol. 17, pp 2343-2348, 2007.

[9] N. Hu, Y. Karube, C. Yan, Z. Masuda and H. Fukunaga, "Tunneling effect in a polymer/carbon nanotube nanocomposite strain sensor" *Acta Materialia* Vol. 56, No. 13, pp 2929-36, 2008.

[10] D. Untereker, S. Lyu, J. Schley, G. Martinez and L. Lohstreter "Maximum conductivity of packed

nanoparticles and their polymer composites" *ACS Appl Mater Interfaces*, Vol. 1, No. 1, pp 97-101, 2009.

[11] L. Liu and J. C. Grunlan, "Clay Assisted Dispersion of Carbon Nanotubes in Conductive Epoxy Nanocomposites" *Adv. Funct. Mater*, Vol. 17, pp 2343-2348, 2007.

[12] J. Sumfleth, X. C. Adroher and K. Schulte, "Synergistic effects in network formation and electrical properties of hybrid epoxy nanocomposites containing multi-wall carbon nanotubes and carbon black" *J Mater Sci*, Vol. 44, pp 3241–47, 2009.

[13] T. D. Fornes and N. D. Huffman, "Method for producing heterogeneous composites" *Patent Application Publication*, US Patent, 2011.

[14] L. L. Lebel, B. Aissa, M. A. El Khakani and D. Therriault "Ultraviolet-assisted direct-write fabrication of carbon nanotube/polymer nanocomposite microcoils" *Adv Mater*, Vol. 22, No. 5, pp 592–6, 2010.

[15] L. Guadagno, B. D. Vivo, A. D. Bartolomeo, P. Lamberti, A. Sorrentino, V. Tucci, L. Vertuccio and V. Vittoria, "Effect of functionalization on the thermo-mechanical and electrical behavior of multi-wall carbon nanotube/epoxy composites", *Carbon*, Vol. 49, pp 1919-30, 2011.

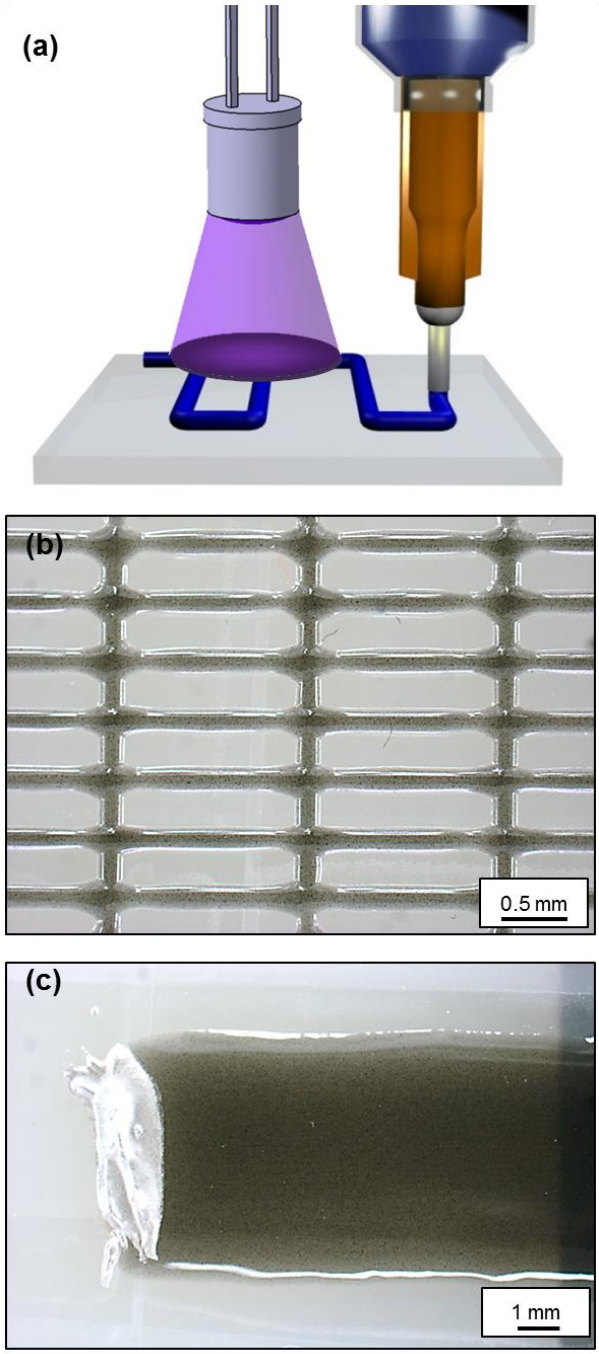

Fig. 1. a) Scheme of UV-DW fabrication of nanocomposite and optical images of b) mesh embedded by the neat polymer and c) nanocomposite thick film.

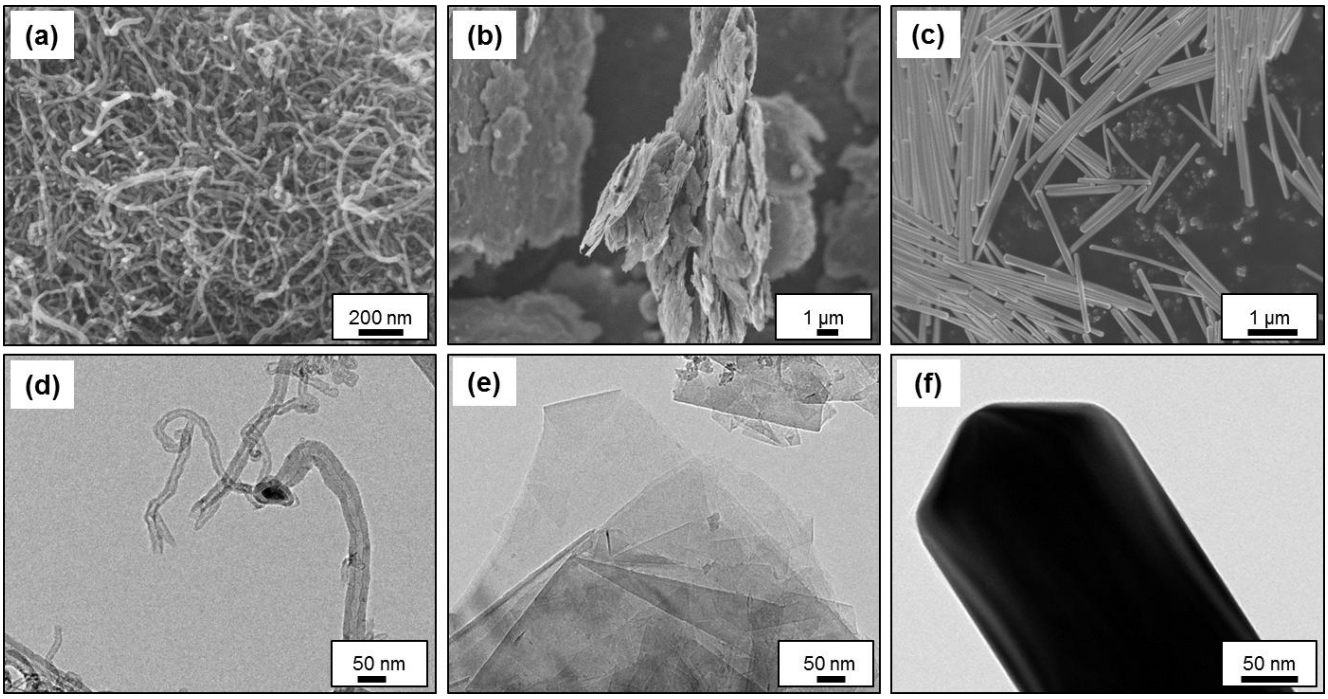

Fig. 2. SEM (a, b and c) and TEM (d, e and f) micrographs of the MWCNTs, the graphene nanosheets and the silver nanowires, used in this study, respectively.

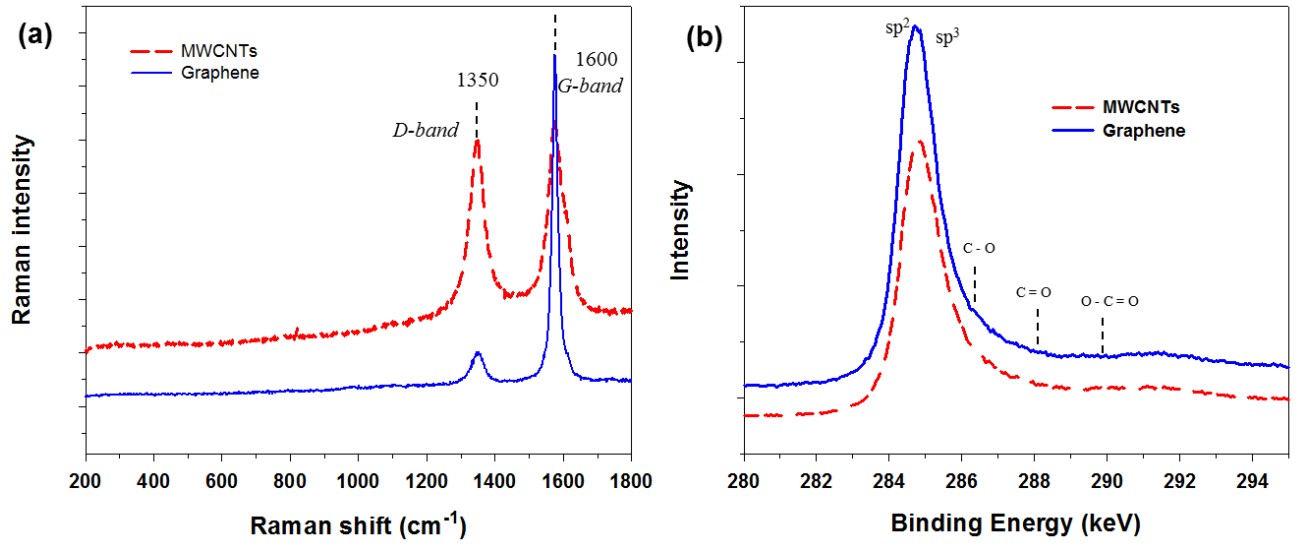

Fig. 3. (a) Raman spectra of MWCNTs (top) and graphene (bottom) and (b) X-ray photoelectron spectra of MWCNTs (bottom) and graphene (top).

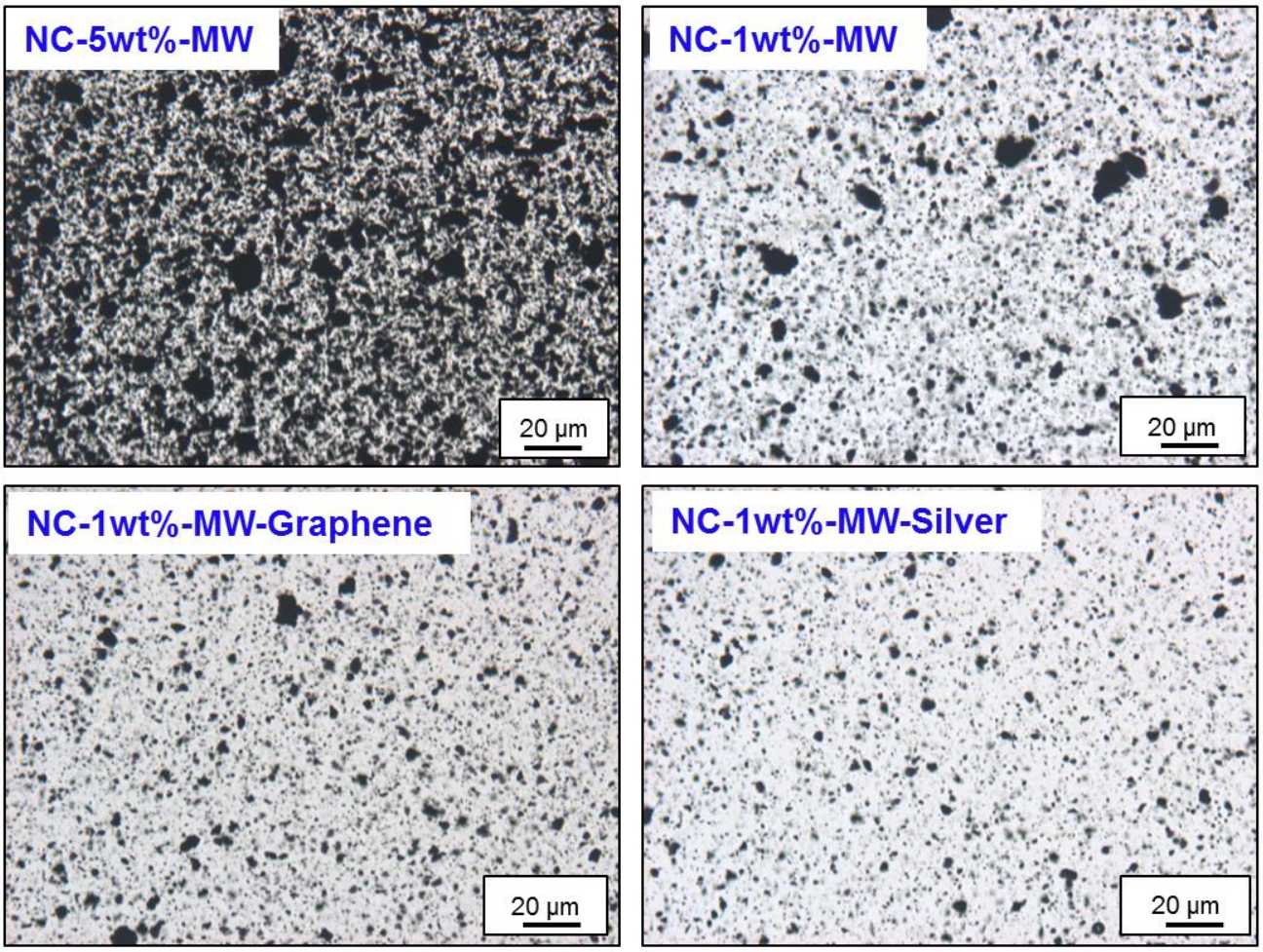

Fig. 4. Optical images of the nanocomposite thick films; (images at the top) the manufactured films made of binary nanocomposites (only MWCNTs as filler) and (images at the bottom) the manufactured films made of ternary nanocomposites (50/50 weight proportion of MWCNTs and graphene or silver nanowire as second filler with the total 1 wt.% fillers concentration).

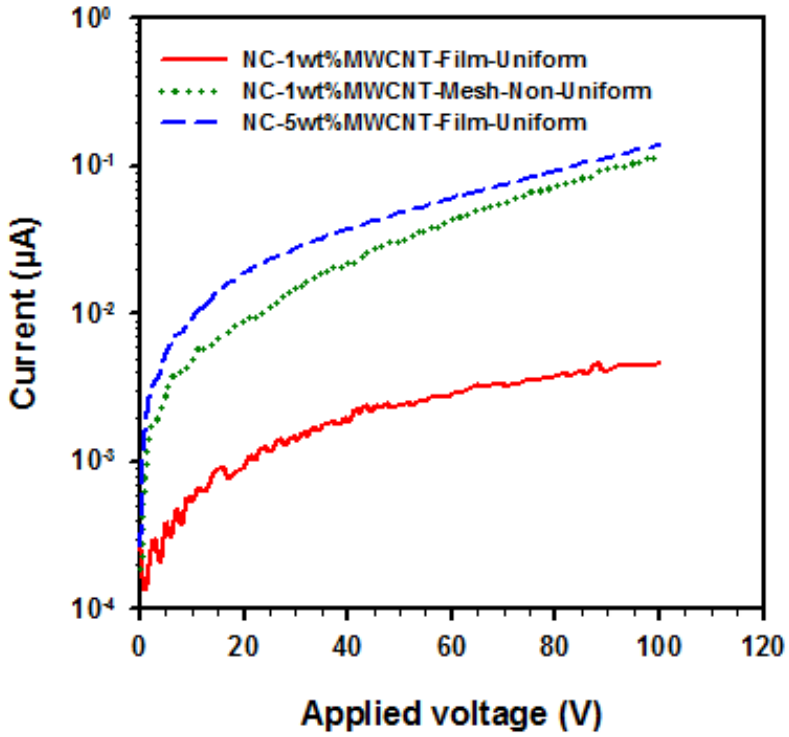

Fig. 5. Measured current upon voltage application (*I-V* curves) of the manufactured nanocomposite mesh (patterned) and the nanocomposite films at 1wt.% and 5 wt.% MWCNTs.

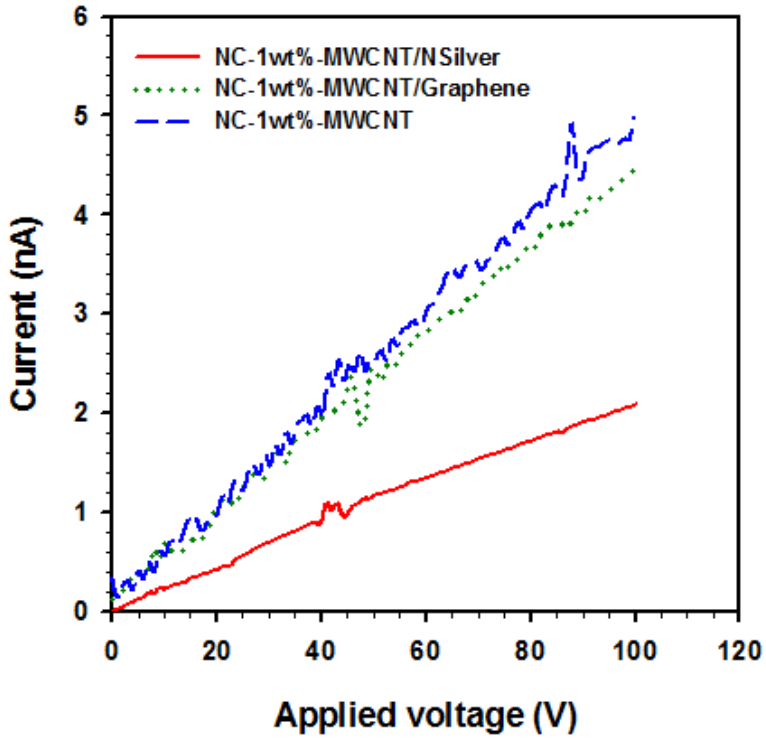

Fig. 6. Measured current upon voltage application (*I-V* curves) of the manufactured nanocomposite films made of binary or ternary systems at total 1wt.% of nanofillers.